AAS 23-228

PERIODIC TRANSFERS THAT DEPART AND RETURN TO AN OPERATING ORBIT USING RESONANT ORBIT STRUCTURES IN THE PLANAR THREE-BODY PROBLEM

Noah I. Sadaka* **and Kathleen C. Howell†**

Many future satellite applications in cislunar space require periodic transfers that shift away from some operational orbit but return. Numerous resonant orbit families in the Earth-Moon Circular Restricted Three-Body Problem (CR3BP) possess a ratio of orbital period to lunar period that is sufficiently close to an integer ratio and can be exploited to uncover periodic transfers. By locating homoclinic connections associated with the operating orbit that incorporate resonant structures, and potentially linking them to resonant orbits, transfers are available for in-orbit refueling/maintenance as well as surveillance/communications applications that depart and return to the same phase in the operating orbit.

INTRODUCTION

As interest in developing infrastructure for cislunar space applications increases, additional capabilities are necessary to create a robust transportation network for spacecraft. One important future capability is refueling or servicing spacecraft already in orbit, an especially critical element for infrastructure development. Spacecraft operating in near-Earth orbits such as Northrup Grumman's Mission Extension Vehicle missions (MEV-1 and MEV-2) have demonstrated that on-orbit maintenance is feasible,[1] and considerable effort is currently being invested to develop component standards and solve hardware design challenges to enable refueling and maintenance by servicing spacecraft.[2] However, the trajectory design aspect for cislunar operations still requires much analysis.

Space surveillance and communications is also an important challenge, i.e. the ability to track the locations of spacecraft in cislunar space and enable inter-satellite communications. Pasquale et al.[3] demonstrate an optimization method for creating constellations of satellites around the Moon based on desired areas of lunar surface coverage. Such a constellation could be paired with a relay satellite, to store data sent from the constellation and to downlink to Earth.

For such applications, an operating orbit serves as a "home base"; departures and arrivals then offer access to wide-ranging destinations. For the servicing and refueling applications, the operating orbit may represent the base orbit for a depot, from which smaller servicing spacecraft (termed servicers) depart to rendezvous with a spacecraft to be serviced (termed the customer). After the servicing operation is complete, the servicer returns and a rendezvous with the depot occurs in the

*Graduate Student, School of Aeronautics and Astronautics, Purdue University, West Lafayette, IN, 47907; nsadaka@purdue.edu.

†Hsu Lo Distinguished Professor of Aeronautics and Astronautics, School of Aeronautics and Astronautics, Purdue University, West Lafayette, IN, 47907; howell@purdue.edu. Fellow AAS; Fellow AIAA.

operating orbit. For a surveillance and/or communications satellite, some flexibility is introduced such that a vehicle remains in an operating orbit for some time and then, periodically, returns to the near-Earth region to downlink acquired data or otherwise engage near-Earth spacecraft. This vehicle then returns to the operating orbit and the same phase at which it departed.

Given the complex gravitational environment in cislunar space, it is reasonable to consider trajectories that leverage these gravitational dynamics in planning scenarios for various applications. Thus, the Circular Restricted Three-Body Problem (CR3BP) is assumed for the preliminary modeling to construct these trajectories as it includes the gravitational influences of both the Earth and the Moon, i.e., the dominant contributors to the gravitational forces in cislunar space. This model is appropriate for the Earth-Moon system during initial trajectory design assessments as the Moon's orbit is nearly circular relative to the Earth.[4] Thus, the dynamical structures in this model are available to be leveraged for real-life mission design in the cislunar region.

Resonant orbits and invariant manifolds with resonant structures emerge as a clear type of bounded motion that serve as a basis to create periodic transfers. Resonant structures offer a variety of geometries and traverse the Earth-Moon system to many destinations. Several previous investigations have also successfully demonstrated the practicality and advantages of using resonant structures for trajectory design in the cislunar environment.[5,6]

THE CIRCULAR RESTRICTED THREE-BODY PROBLEM

The Circular Restricted Three-Body Problem (CR3BP) is a time-independent model that describes the motion of a particle with negligible mass, labelled P_3, in a gravitational potential formed by two spherically-symmetric massive bodies. In this model, the massive bodies, termed the primaries and denoted P_1 and P_2 for the larger and smaller mass, respectively, move in circular orbits about their common barycenter. Any CR3BP system is characterized by the mass ratio $\mu = \frac{M_2}{M_1+M_2}$ for the primaries, where M_1 and M_2 are the masses of P_1 and P_2, respectively. For the Earth-Moon CR3BP, this mass ratio is approximately $\mu = 0.0121506$. The motion in this model is governed by three second-order differential equations, expressed in a barycenter-centered frame that rotates with the primaries. The coordinate axes for this rotating frame are defined by an $\hat{x} - \hat{y} - \hat{z}$ dextral orthonormal triad, viewed in teal in Figure 1, where the $\hat{x}$ axis is directed from P_1 to P_2, the $\hat{z}$ axis is parallel to the orbital angular momentum vector for the orbit of the primaries, and $\hat{y}$ completes the right-handed triad. The orientation of the rotating frame with respect to an inertial frame at a certain time is defined by the angle θ in Figure 1. The CR3BP equations of motion are non-dimensionalized to generalize the model and reduce numerical error. The characteristic quantities are defined as the distance between the primaries l^*, the total mass of the system, $m^* = M_1 + M_2$, and the characteristic time t^* is selected such that the mean motion $\dot{\theta}$ for the primaries relative to the barycenter B is equal to 1. This non-dimensionalization of the problem variables results in the distance between the primaries being equal to 1 and the locations of P_1 and P_2 on the $\hat{x}$-axis being equal to $-\mu$ and $1-\mu$, respectively. The resulting equations of motion for the six-dimensional state for P_3, $\vec{r} = [x, y, z, \dot{x}, \dot{y}, \dot{z}]$, are

$$\ddot{x} = 2\dot{y} + \Omega_x \tag{1}$$

$$\ddot{y} = -2\dot{x} + \Omega_y \tag{2}$$

$$\ddot{z} = \Omega_z \tag{3}$$

where Ω_i is a partial derivative of the pseudo-potential function Ω with respect to each of the position

components, i,

$$\Omega = \frac{1-\mu}{\|\vec{R}_{13}\|} + \frac{\mu}{\|\vec{R}_{12}\|} + \frac{x^2+y^2}{2} \tag{4}$$

as evident in Figure 1, $\vec{R}_{12}$ and $\vec{R}_{13}$ are the respective position vectors from P_1 and P_2 to P_3. (Note that arrow overbars indicate vectors.)

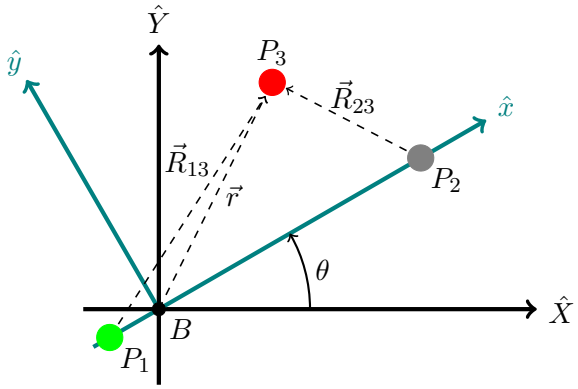

Figure 1: The CR3BP rotating frame

This investigation is focused on trajectories in the Planar CR3BP (PCR3BP), where all motion occurs in the Earth-Moon orbital plane and thus $z = 0$ in the equations of motion. Five equilibrium solutions, denoted the Lagrange points, exist in this model. The collinear Lagrange points, i.e., L_1, L_2, and L_3, are all located along the $\hat{x}$-axis. The equilateral Lagrange points L_4 and L_5 are off the $\hat{x}$-axis but form equilateral triangles with the primaries.

No analytical solution exists in the CR3BP, however, one integral of motion is available i.e., the Jacobi Constant (JC). This integral of the motion represents an energy-like quantity and is evaluated for any state as

$$JC = 2\Omega - (\dot{x}^2 + \dot{y}^2 + \dot{z}^2)) \tag{5}$$

of course, JC remains constant along any ballistic arc. Equation (5) is rearranged to solve for the resulting velocity magnitude at a given position and for a specified JC level. Locations with zero rotating velocity define the zero-velocity curves (ZVC) for the PCR3BP. These curves bound the possible motion of a trajectory.

PERIODIC ORBITS

Periodic orbits are a type of repeating motion in the CR3BP where a trajectory returns to its initial state after some period, T. These solutions provide structure in an otherwise complex dynamical environment and are frequently leveraged as predictable behavior for trajectory design. While the CR3BP is a lower-fidelity model, only including the two largest contributors to the gravitational force on a spacecraft, analysis in the CR3BP is adequate as orbits and trajectory arcs are generally successfully transitioned to a high-fidelity $\mathcal{N}$-body model.[7] Leveraging CR3BP-based structures served as the basis for design in numerous space missions, e.g.,the Earth-Moon distant retrograde orbit incorporated during the Artemis I mission[8] and the 2:1 spatial resonant orbit that is the current orbit for the Transiting Exoplanet Survey Satellite (TESS).[9]

Periodic orbits are constructed by propagating an appropriate initial state and using a corrections algorithm to deliver periodicity. Given one periodic orbit, families of orbits are generated by varying one parameter (such as the x-position associated with a perpendicular crossing) and using a continuation process.

Useful insights result from the application of dynamical systems theory to the CR3BP, including orbital stability information. The State Transition Matrix (STM) associated with the equations of motion provides a linear estimate of the variation in the final states due to a perturbation in the initial states. For a periodic orbit, the STM evaluated after exactly one period is termed the monodromy matrix; that is, a stroboscopic map of the variation in the states analyzed using discrete-time systems theory. As this model is a Hamiltonian system, the six eigenvalues λ_i of the monodromy matrix occur in three reciprocal pairs and describe the linear stability of an orbit. An orbit is considered stable if all $|\lambda_i| \leq 1$ and unstable if any eigenvalue $|\lambda_i| > 1$. The eigenvectors associated with an unstable eigenvalue and its reciprocal pair are exploited to numerically generate invariant manifolds. Invariant manifolds are successfully employed in numerous other investigations to generate low-cost transfers and to explore the dynamical relationships between periodic orbits.[10,11]

Resonant Orbits

In the Earth-Moon CR3BP, a vehicle in a resonant orbit possesses an orbital period that is commensurate with the period of the lunar orbit.[12] The ratio of orbital periods is typically expressed as a $p : q$ resonance, where in the Earth-Moon system, p represents the number of revolutions of the spacecraft around the Earth and q is the number of revolutions of the Moon around the Earth. In an Earth-centered Kepler problem, the Moon does not impart any gravitational influence and, therefore, a resonant orbit is defined by an exactly integer resonance ratio. However, the addition of the lunar gravitational effects for resonant orbits to the CR3BP results in the resonance ratio being close to, but not exactly, a precisely integer ratio.[12]

Exterior resonant orbits are defined when $p < q$ and, for interior resonant orbits, $p > q$. The variety of resonance ratios and the different characteristics of interior and exterior resonant orbits provides a wide range of orbit geometries. One of the advantages of using resonant structures for transfer design is that the pathways collectively traverse through large swaths of space as apparent in Figure 2, where a set of resonant orbits is plotted at several energy levels along with the corresponding ZVCs. Resonant orbits reach a variety of useful locations throughout Earth-Moon space, including regions near the primaries, the collinear Lagrange points, the equilateral Lagrange points, and the exterior region of the system. Notably, the availability of different resonant orbits depends on the selected energy level, with many exterior resonant orbits only available at lower values of Jacobi Constant. These values of JC are associated with ZVC bounds that restrict access to certain regions, for example the Moon may not be accessible if the L_1 gateway is closed. However, the large variety of geometries offered by resonant orbits are an attractive option for many space infrastructure applications and as operating orbits for satellites.

The selection of a specific resonant orbit is based on information represented by the resonance ratio. The values for p and q are expressed as the number of revolutions around the Earth as viewed by an inertially-fixed observer. Therefore, the orbit is propagated for p revolutions to yield an orbit that is periodic in the rotating frame. Once an appropriate conic orbit is generated, different strategies are employed to transition the orbit to the CR3BP.[13] A converged $p : q$ resonant orbit in the CR3BP then seeds a differential corrections process to construct a family of $p : q$ resonant orbits.

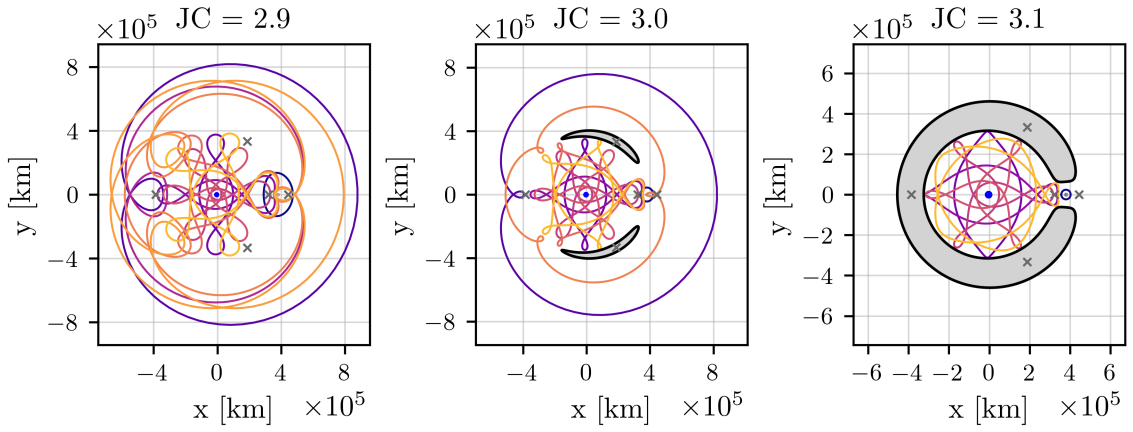

Figure 2: Several resonant orbits plotted at different energy levels. The locations of the Lagrange points are marked with crosses and the ZVCs appear as black curves. Regions that are inaccessible appear with grey fill

Phasing is an important consideration in the design of periodic transfers and resonant orbits emerge as an appropriate type of trajectory for phasing constraints. Some families of resonant orbits possess a range over which the period of various members within the family do not vary significantly.[13] This period is also frequently close to the expected resonant period of $T_{res} = 2\pi q$. For example, the 2:3, 5:3, and 2:1 resonant orbit families are plotted in Figure 3, and colored by the fraction of actual period T to the resonant period T_{res}. A large proportion of each family possess periods that are very close to the resonant period as illustrated by the T/T_{res} ratios that are close to one, thus, the periods of these members are predictable and the orbits are applicable for periodic transfer design. However, as noted by Anderson et al.,[13] orbits that loiter near the smaller primary over extended intervals results in larger deviations between the orbit period and the resonant period, a phenomenon that is apparent for the 2:3 resonant orbit family plotted in Figure 3(a).

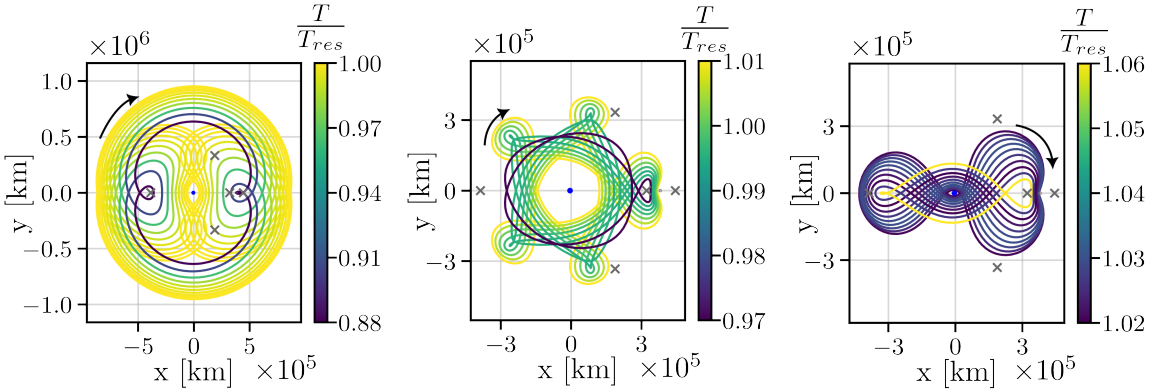

(a) 2:3 resonant orbit family (b) 5:3 resonant orbit family (c) 2:1 resonant orbit family

Figure 3: Members of resonant orbit families colored by the fraction of orbital period to resonant period $\frac{T}{T_{res}}$

An attribute of many prograde resonant orbits, including those appearing in Figure 3, are the "loops" at apses that appear when viewed in the CR3BP rotating frame. These loops are a result of the variation in the orbit's rotating velocity with respect to the angular velocity of the primaries. Interior resonant orbits have loops at their apoapses pointing outwards, and exterior resonant orbits have loops at their periapses pointing inwards. The locations and velocity directions of these loops are exploited to reach desired locations in space when designing periodic transfers.

Lyapunov Orbits

An advantage of multi-body gravitational models, such as the CR3BP, is the emergence of equilibrium solutions that serve as a source of periodic behaviors. Various libration point orbits (LPO) exist in the vicinity of their respective Lagrange points, and include the planar Lyapunovs and their spatial counterpart, the halo families of simply symmetric orbits. These orbits are successfully leveraged for mission design in the Earth-Moon system and are candidate orbits for lunar surveillance missions[14] and cislunar depot locations.[2] This investigation is focused on members of the L_1 and L_2 planar Lyapunov orbit families; a subset is plotted in Figure 4 from which one is selected as the operating orbit. The L_1 and L_2 Lyapunov orbits that are plotted in Figure 4 are linearly unstable and their invariant manifolds appear in previous investigations as the basis to design low-cost transfers.[5] The presence of manifolds implies that L_1 and L_2 orbits are attractive for an operating orbit as many natural departure and arrival paths are available to be leveraged to explore cislunar space.

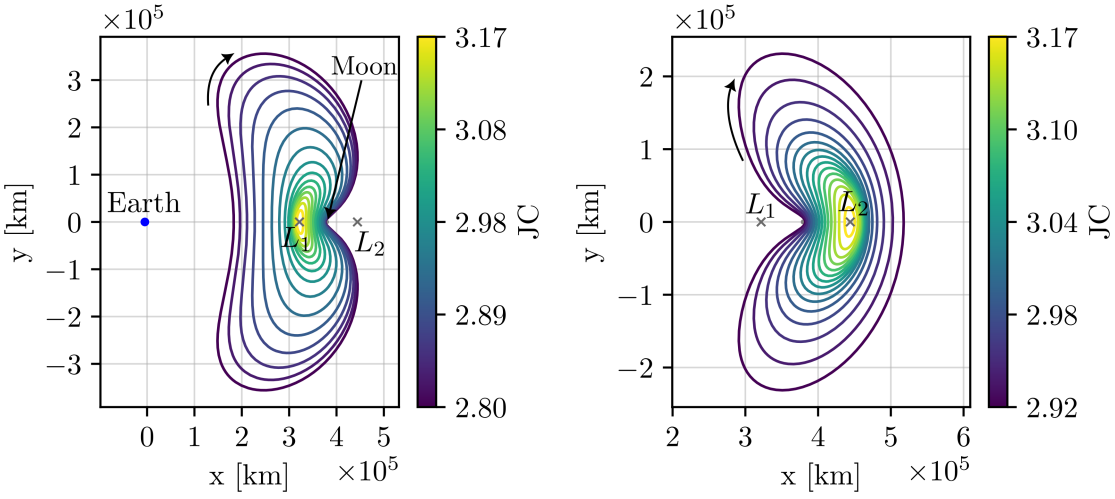

(a) Members of the L_1 Lyapunov family

(b) Members of the L_2 Lyapunov family

Figure 4: L_1 and L_2 Lyapunov orbit families in the Earth-Moon system

The third collinear Lagrange point, L_3, is also the source for a family of Lyapunov orbits as plotted in Figure 5. Notably, these L_3 Lyapunov orbits are in 1:1 resonance with the Moon, and are constructed in the Earth-Moon system using either the typical linearization technique employed for the L_1 and L_2 Lyapunov orbits[4] or by generating an appropriate 1:1 resonant conic orbit and transitioning it to the CR3BP. As this orbit family is located on the opposite side of the Earth as compared to the Moon, the members plotted in Figure 5 do not spend significant time (if any) near the Moon and, therefore, its period does not vary significantly from the 1:1 resonance ratio.

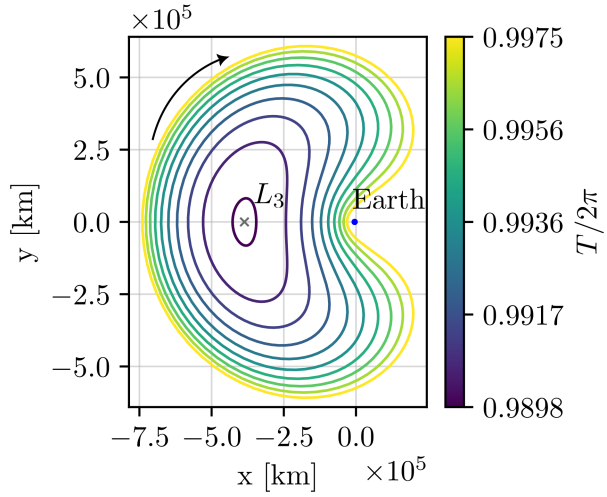

Figure 5: Members of the L_3 Lyapunov family colored by the period over 2π

GENERATING PERIODIC TRANSFERS

Invariant manifolds provide natural transfers paths that asymptotically depart from the operating orbit and return without any propellant expenditure; an attractive option for a servicing spacecraft as propellant can be conserved for a refueling operation. Homoclinic connections, a special type of invariant manifold arcs where an unstable arc flows into a stable arc, are investigated as a basic framework to freely shuttle spacecraft throughout space to accomplish mission objectives.

Figure 6 includes a schematic for a transfer design strategy. A symmetric homoclinic connection with propagation time $2T_{man}$ is generated from the operating orbit with period T_O and with a manifold insertion location at time τ, as measured from a perpendicular crossing of the orbit. The homoclinic connections with resonant structures are explored, offering potential transfers into a periodic orbit at a common perpendicular crossing with period T_{PO}. Transferring into a periodic orbit allows for greater flexibility in designing periodic trajectories originating from the operating orbit. For example, a servicing or on-orbit refueling could occur in such an orbit, where both the servicer and customer rendezvous and remain for one or more periods along the orbit before the return of the servicer to the operating orbit. To identify a periodic transfer path, the fraction $\mathcal{Q}$ is defined as the sum of the time-of-flight for each segment along the transfer over the period of the operating orbit. Periodic transfers are produced when $\mathcal{Q}$ is an integer, that is,

$$\mathcal{Q} = \frac{n_{PO}T_{PO} + 2T_{man} + 2\tau}{T_O} \tag{6}$$

where n_{PO} is an integer representing the number of revolutions to remain in the periodic orbit before returning to the operating orbit via the homoclinic connection. For a scenario where no transfer to a periodic orbit is planned, n_{PO} is zero.

Constructing Natural Transfers to/from the Operating Orbit with Resonant Structures

The use of homoclinic connections to depart from and return to the operating orbit is desirable as these trajectories supply propellant-free transfers. Invariant manifold structures in the CR3BP also provide insight into the dominant dynamical flows in a gravitational environment dominated

by two massive bodies. Once a suitable unstable L_1 or L_2 Lyapunov is identified for the operating orbit, its invariant manifolds are generated and homoclinic connections with desirable structures are identified for the construction of periodic transfers.

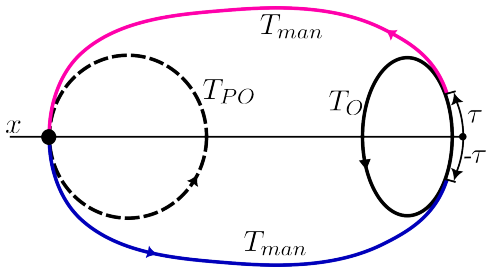

Figure 6: Periodic transfer schematic

To approximate the invariant manifold surfaces, manifold arcs from many fixed points are propagated. Visualizing manifold surfaces is challenging, therefore, a Poincaré section is defined with a hyperplane at $y = 0$ and the impinging of trajectories on that map is analyzed. This dimensionality-reduction technique allows the full four-dimensional state to be visualized on a two-dimensional map; by constraining one dimension with the location of the hyperplane, and with all manifold arcs possessing the same Jacobi Constant value as their generating orbit, points that appear close by on the Poincaré section are near each other in the four-dimensional space. This property is especially useful in converging homoclinic connections; stable and unstable manifold arc intersections on the map that are close to one another are used as initial guesses in a robust differential corrections scheme and corrected for continuity.

Symmetric homoclinic connections yield perpendicular crossings (PC) in a solution and reduce the complexity for locating candidate homoclinic connections for periodic transfers. Exploiting symmetric structures reduces the computation time to converge to a homoclinic connection, given that only one half of the path requires correction. The corrections scheme appears in Figure 7, where the step-off offset distance d to numerically construct a manifold occurs after time τ along the orbit as measured from a perpendicular crossing along the generating orbit. A manifold arc constraint developed by Haapala and Howell[10] ensures that the arc remains on the operating orbit's manifold. The manifold arc selected from the Poincaré map is discretized into n segments with respective propagation times T_i and intermediate arcs are constrained for continuity. The final state $\vec{x}_n^{'}$ along the terminal arc is constrained to be a perpendicular crossing.

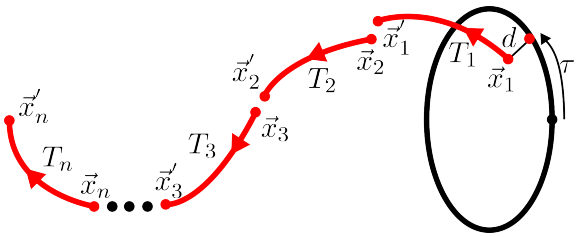

Figure 7: Symmetric homoclinic connection targeter schematic. Adapted from Haapala and Howell[10]

Predicting the existence of homoclinic connections that incorporate resonant structures are demonstrated by Vaquero and Howell;[15] numerous examples are produced as well. By identifying manifold arcs for the operating orbit that pass near the fixed points representing the resonant orbits on a Poincaré section, homoclinic connections with structures similar to nearby resonant orbits are often observed. Invariant manifolds for the operating orbit that are aligned with resonant structures take advantage of both the natural departure and arrival properties of invariant manifolds and the geometrical and timing properties of resonant orbits. The resulting transfer reflects a resonant structure where clear geometrical elements from the associated resonant orbit are apparent, e.g., the number and location of apses. The osculating period for the transfer is also close to the resonant orbital period. An example highlighting these properties is plotted in Figure 8 for a transfer corresponding to $JC = 3.02261$. An intersection of the stable and unstable manifolds for the L_2 Lyapunov orbit that pass near a fixed point of the 5:3 resonant orbit at the same energy level are identified on the map in Figure 8(a). This initial guess is corrected to result in the homoclinic connection plotted in red in Figure 8(b) that shares many geometrical elements with the 5:3 resonant orbit plotted with a dashed green line. The ratio of osculating period T_{osc} to Lunar period T_{moon} for the transfer is plotted in Figure 8(c) with the black dashed line highlighting the precise resonant ratio of $\frac{3}{5}$ for a 5:3 resonant orbit. Note that the osculating period tends to infinity at the start and end of the transfer as the osculating orbit is hyperbolic near the L_2 Lyapunov orbit.

One advantage of employing L_1 and L_2 Lyapunov orbits as an operating orbit is their existence across many energy levels that then yield many different homoclinic connections that exhibit resonant structures.[16] The homoclinic connections for these orbits flow in close vicinity to the structure existing in the periodic orbits. Given innumerable unstable resonant orbit families, many homoclinic connections emanating from L_1 and L_2 orbits also incorporate resonant structure.

Continuing Homoclinic Connections and Converging Periodic Transfers

A given homoclinic connection is unlikely to be exactly periodic with the motion in the operating orbit. Prior knowledge of the time-of-flight for the homoclinic connection, as well as a known value for the period of an orbit, is required to evaluate $\mathcal{Q}$ in Equation (6) and assess if it is an integer value. However, the necessity for the numerical correction and propagation of trajectories to evaluate Equation (6) results in a homoclinic connection as identified from a Poincaré section that is not necessarily periodic.

With the challenges in constructing the appropriate links, the homoclinic connections are continued into a family of transfers that all possess the same underlying structures to enable the determination of periodic members. Casoliva et. al.[16] show that homoclinic connections exist in one-parameter families. For this analysis, *natural parameter continuation* is sufficient to generate such a family. The corrections scheme in Figure 7 employs a fixed Jacobi Constant value for the operating orbit, thus, by monotinically varying the Jacobi Constant value for the operating orbit and using the previously-converged homoclinic connection as an initial guess, the same corrections strategy is applied, producing a new homoclinic connection for this new operating orbit. Each member in the family is, therefore, a ballistic transfer at some Jacobi Constant value to and from an operating orbit defined at the same Jacobi Constant value and yet conserves the desired resonant structure apparent in the initial homoclinic connection. For example, the transfer in Figure 8(c) is continued and plotted in Figure 9(a), where the 5:3 structure of all the members of the family is maintained.

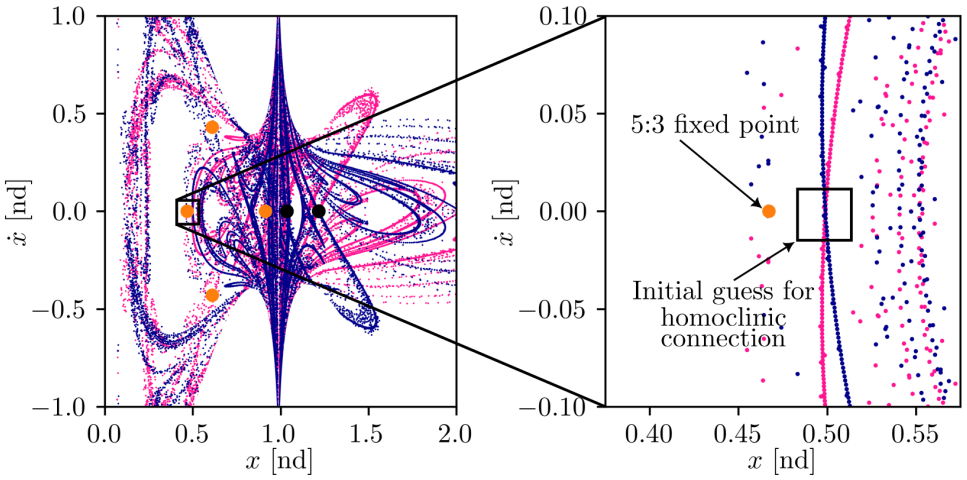

(a) $y = 0$ Poincaré section generated from 5000 fixed points evenly spaced in time around the orbit, a step-off distance of 40km, and a propagation time of 173.7 days

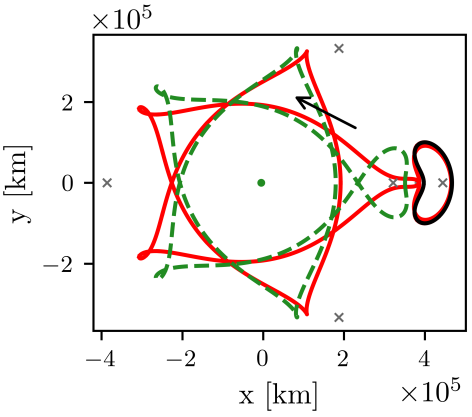

(b) The transfer (red) viewed in configuration space along with a 5:3 resonant orbit (green, dashed) and generating L_2 Lyapunov (black)

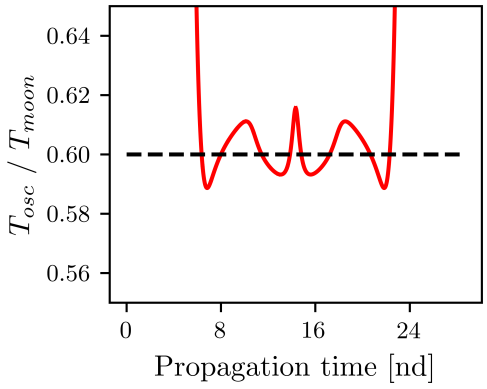

(c) The osculating resonance ratio of the transfer (red) and the 5:3 perfect resonant ratio (black, dashed)

Figure 8: (a) Poincaré section with unstable (pink) and stable (dark blue) manifold arcs. Fixed points for the 5:3 resonant (orange) and L_2 Lyapunov (black) orbits are marked. (b, c) Recognizing the existence of resonant structures in a homoclinic connection

Once a family of homoclinic connections is generated, Equation (6) is evaluated across the family to identify members that produce a periodic transfer. The time-of-flight for the different segments comprising the transfer, including the period for a periodic orbit with a perpendicular crossing location that is the same as the symmetric homoclinic connection, must be evaluated for each member. Equation (6) is evaluated across the family in Figure 9(a) and is plotted in Figure 9(b). A periodic transfer is identified with a period equal to 9 revolutions of the L_2 Lyapunov operating orbit with $JC = 3.067$. As the period of the potential operating orbits, the homoclinic connection, and the destination periodic orbit all vary smoothly throughout the family, Equation (6) is evaluated for evenly-spaced values in JC. Such a process occurs along a subset of the family and the periodic solutions are identified using a bracketing iterative method.

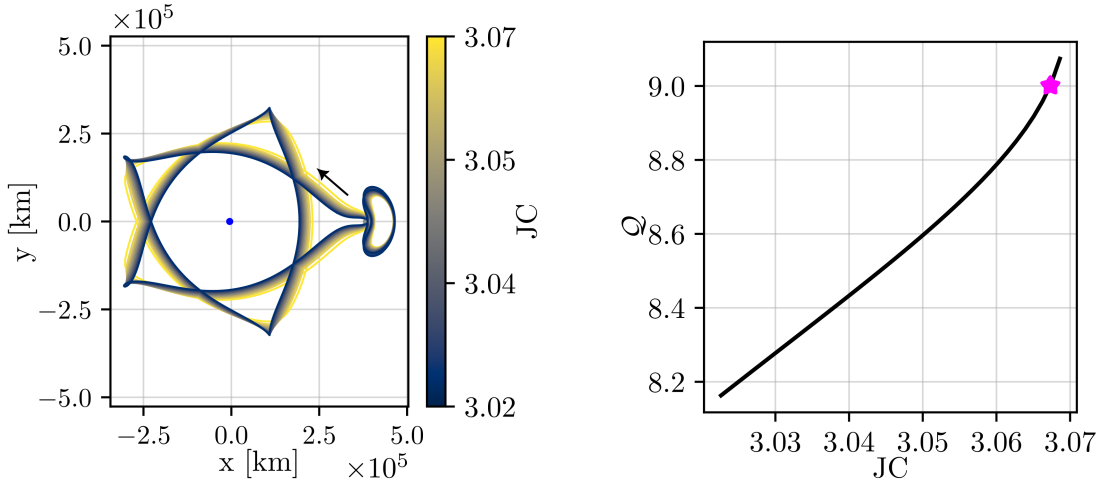

(a) Family of ballistic transfers from L_2 Lyapunov orbit with 5:3 resonant structure

(b) Equation (6) evaluated along the family. A periodic transfer is identified with a star

Figure 9: Identifying a periodic transfer with 5:3 resonance structure from a L_2 Lyapunov operating orbit

Defining the time-of-flight for a manifold arc T_{man} is challenging due to the asymptotic nature of invariant manifolds. The same manifold arc can be reached from any location along the orbit by varying the step-off distance d, and monotinically decreasing d eventually results in the manifold arc "wrapping" around the orbit for an additional revolution, adding T_O to T_{man}. Therefore, the transfer time T_t departing from the operating orbit is defined as equal to $T_t = nT_O + 2T_{man} + 2\tau$, where n is either zero, a positive integer, or a negative integer assuming that the manifold does not depart the orbit. Then, T_{man} and τ are defined based on the selected step-off distance; for this analysis $d = 40$km. Once a periodic transfer is achieved, increasing the numerator in Equation (6) by nT_O does not influence the periodic properties for the transfer, as $\mathcal{Q}$ remains an integer. Thus, transfer time-of-flight is defined to be the time-of-flight using a step-off distance $d = 40$km, however, nT_O can be added to this time if a smaller offset distance is preferred.

PERIODIC TRANSFERS FOR CISLUNAR INFRASTRUCTURE DEVELOPMENT

Periodic transfers are potentially useful for a variety of important applications in cislunar space to support future development of the region. Several examples are showcased to demonstrate the versatility of resonant orbits and resonant structures in transfer design and to evaluate periodic transfers for application to different mission scenarios. Transfers that are comprised solely of homoclinic connections are first demonstrated followed by periodic transfers that deliver a vehicle into a resonant orbit for a servicing scenario. Finally, sample transfers that reach L_3 Lyapunov orbits from the Lunar region are introduced.

Homoclinic Connections as Transfer Options

One prominent example that leverages the dominant dynamical motion in the CR3BP for a spacecraft servicing application was originally proposed by the National Aeronautics and Space Administration (NASA) Goddard Space Flight Center (GSFC), termed the LOTUS framework.[2] This

framework planned for a space telescope, originally in an orbit in the vicinity of Sun-Earth L_2, to rendezvous with a servicing depot in an Earth-Moon L_1 Lyapunov operating orbit. Both vehicles then transfer into a "highly elliptical" orbit around the Earth that requires minimal propellant use for each; then, a human crewed vehicle meets up with the telescope and depot stack at an apse and subsequently returns to Earth after the servicing operation is completed.[2] The space telescope and depot then transfer back to the operating orbit with a relatively small impulse.[2] The original transfer is viewed in Figure 10(a) and appears to be leveraging an 8:3 resonance structure with an energy level near $JC = 3.15$; the small maneuvers required to leave from and arrive into the operating orbit implies the use of invariant manifold structures. A similar structure is successfully constructed in the CR3BP and is plotted in Figure 10(b), where the transfer time equals 8.74 revolutions of the operating orbit. Using this initial transfer to construct a family, the periodic transfer shown in Figure 10(c) emerges, with a Jacobi Constant value of 3.0903 and a transfer time of 110.93 days, corresponding to exactly eight 13.87-day revolutions of the operating L_1 Lyapunov orbit.

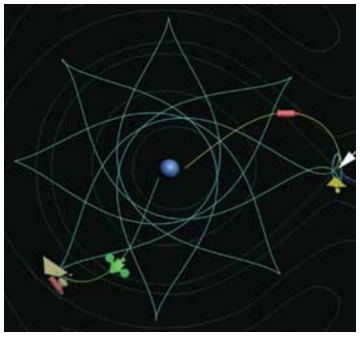

(a) LOTUS framework, adapted from 2021, *On-Orbit Satellite Servicing Study: Project Report*, NASA GSFC.[2]

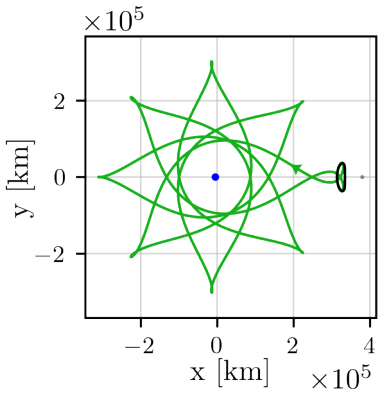

(b) L_1 at JC=3.15 homoclinic connection with 8:3 resonance.

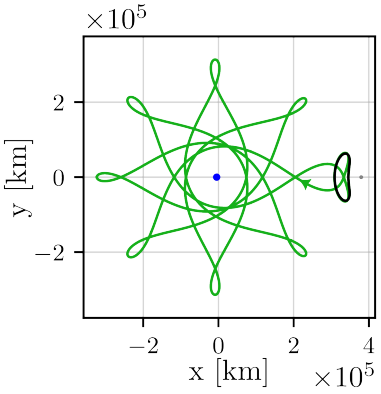

(c) Periodic LOTUS-like transfer with JC=3.0903.

Figure 10: The LOTUS framework

This periodic transfer maintains the mission requirements from the NASA study while permitting new capabilities and mission types. One of the initially stated objectives for this framework included an orbit that is easily accessible from Earth. Such a constraint is possible due to the numerous apses in the 8:3 resonance structure used for an insertion into and departure from the LOTUS, a property retained by the periodic transfer. The applicability of this trajectory framework is extendable to create a depot resupply framework by inserting a spacecraft into the LOTUS at one of the apses and a natural rendezvous occurs with the depot that remains in the operating orbit.

Certain types of missions scenarios benefit from the ability to occasionally depart from their operating orbit and allow closer passes of the Earth to downlink data or interface with satellites in that region. For example, science missions near the Moon could return to downlink data closer to the Earth and reduce their reliance on the Deep Space Network. Similarly, space surveillance satellites that complete observations in their operating orbit could then potentially transfer to the near-Earth region for data transmission. Transfers that make close passes of the Earth offer paths for spacecraft launched from Earth or temporarily stationed near it to originally insert into their operating orbit as well. Therefore, resonant structures that include close approaches of the Earth are considered for periodic transfer design.

Several resonant orbits have members that pass near the Earth, such as the 2:1 family plotted in Figure 3(a). Gupta et. al[6] identify cislunar surveillance applications for this family of orbits, as spacecraft in a 2:1 resonant orbit potentially interface with satellites in LPOs near the Moon, observe the Lunar region including the Lunar far side, and periodically reach low Earth altitudes. The members of the 2:1 resonant orbit family with periapses very close to the Earth possess high energies with values of $JC =\approx 2.2 - 2.6$, i.e., much higher than those for the L_1 and L_2 Lyapunov orbits typically considered for Lunar operations and plotted in Figures 4(a) and 4(b), thus, it is unlikely that homoclinic connections with a 2:1 structure exist for these Lyapunov orbits such that a pass very close to the Earth occurs. However, homoclinic connections can still be constructed that retain the 2:1 resonance structure and pass near the Earth, as apparent in the periodic transfer from a L_1 Lyapunov plotted in Figure 11. The Jacobi Constant for this transfer is $JC = 2.9135$, a relatively high energy level for the L_1 Lyapunov family, but this transfer includes two periapses at an Earth altitude of 88239km. The time-of-flight for this transfer is 140.72 days, significantly longer than the expected 2:1 resonance period of 1 sidereal month, i.e. 27.28 days, due to the manifold arcs wrapping several revolutions of the operating orbit (a period of 28.14 days), to depart and arrive. These details are consistent with the higher-energy L_1 Lyapunov orbits that are less unstable than the lower-energy members of the family.[14]

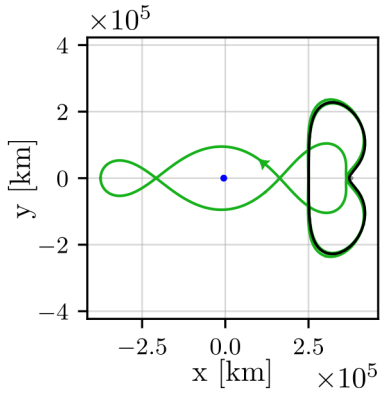

Figure 11: Periodic transfer with 2:1 structure from L_1 Lyapunov at JC =2.9135

If closer approaches of the Earth are desired, 3:1 resonance structures are available. As apparent in Figure 12, for the same Jacobi Constant value, a 3:1 resonant orbit more closely approaches the Earth than a 2:1 resonant orbit, such that lower altitude Earth orbits are accessible at a lower energy level. For this example, a L_2 Lyapunov orbit is selected as the operating orbit, although similar 3:1 geometries also exist for a L_1 Lyapunov. The periodic transfer with a 3:1 resonance structure is plotted in Figure 13(a). This homoclinic connection includes some additional structure that links the L_2 Lyapunov to the 3:1 resonant structure, but the resonant geometry is clearly present and comparable to the 3:1 resonant orbit plotted at the same Jacobi Constant level of $JC = 3.03258$ in Figure 13(b). This transfer includes three close approaches of the Earth, with the periapse on

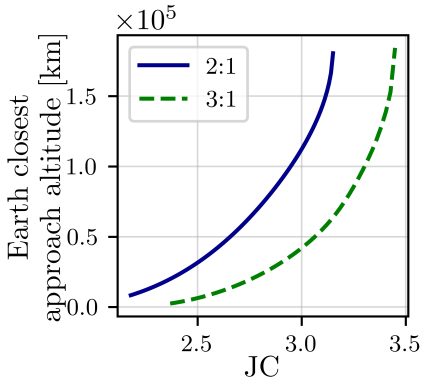

Figure 12: Earth closest approaches for 2:1 and 3:1 resonant orbit families

the $x-$axis at an altitude of 42555km above the Earth and the off-axis periapses with altitudes of 44658km, that is, around 10000km above the GEO altitude. The time-of-flight for this transfer is 176.53 days, and the operating orbit has a period of 17.65 days.

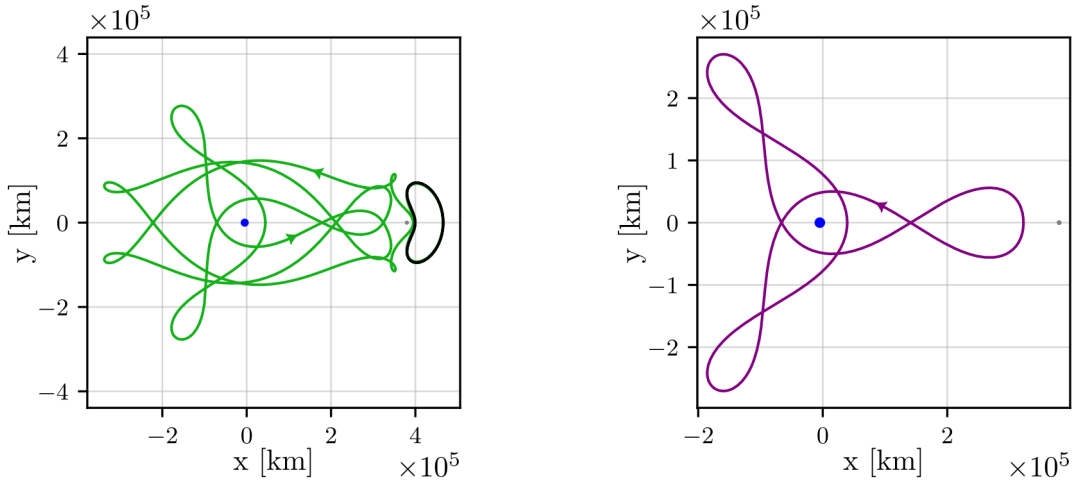

(a) Periodic transfer with 3:1 structure from L_2 Lyapunov at $JC = 3.03258$

(b) 3:1 resonant orbit at $JC = 3.03258$

Figure 13: Transfers for near-Earth approaches

Resonant Orbits as Destinations

Homoclinic connections with resonant structure can enable low-cost periodic transfers into periodic orbits. For a servicer and depot application, assume that the depot remains in the operating orbit and the servicer departs to service a customer on a different periodic orbit. The homoclinic connection serves as the mechanism for the servicer to freely depart and return to the operating orbit while shuttling the servicer to an appropriate location in space such that it transfers onto and then off from the destination orbit after some specified n_{PO} revolutions.

For example, in Figure 14, a periodic transfer from an L_2 Lyapunov operating orbit, with $JC = 3.0352$, into a 5:3 resonant orbit using a homoclinic connection with 5:3 resonance structure is plotted. The common perpendicular crossing between the homoclinic connection and the destination orbit, identified with a black star, is used to insert onto the orbit and then to depart it to return to the operating orbit along the homoclinic connection. The cost to transfer between the homoclinic connection and the resonant orbit is $\Delta v = 12.35 m/s$, for a total cost of $\Delta v = 24.7 m/s$ over the entire transfer. The servicer spends one revolution along the 5:3 resonant orbit, with a Jacobi Constant of $JC = 3.0593$ and a period of 81.4 days, before returning to the operating orbit, for a total time-of-flight of 227.86 days or 13 revolutions of the 17.52-day operating orbit.

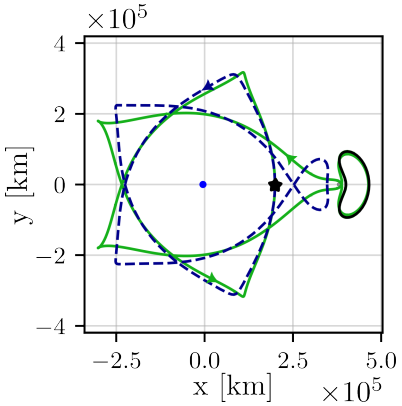

Figure 14: Periodic transfer from an L_2 Lyapunov orbit (black) to a 5:3 resonant orbit (blue, dashed) using a homoclinic connection with 5:3 resonance structure (green)

The low transfer cost is enabled by the similarity in structure between the homoclinic connection and the resonant orbit. Both the homoclinic connection and resonant orbit possess similar osculating periods at their common perpendicular crossing – a distance r from the Earth – where a conic approximation for the velocity is $v_{2bp} = \sqrt{c(2/r - 1/(c(T_{osc}/(2\pi))^2)^{1/3})}$, with c defined as the Earth's gravitational parameter and v_{2bp} is expressed in an Earth-centered inertial frame. The velocity in the CR3BP does not exactly equal v_{2bp} due to the Lunar gravitational influence, however, the similarity in the osculating period ensures that the homoclinic connection and resonant orbit compare similar velocities; a burn at a perpendicular crossing ensures that the velocity directions are aligned, contributing to a low-cost transfer.

An even lower cost periodic transfer appears in Figure 15 where a L_2 Lyapunov operating orbit reaches a customer on a 2:3 resonant orbit by means of a homoclinic connection with a 2:3 resonance structure. This transfer has a total cost of $\Delta v = 14.24 m/s$ with a time-of-flight of 258 days, corresponding to 10 revolutions of the 25.8-day operating orbit. The energy level for the operating orbit is $JC = 2.9492$ and the energy level for the customer orbit is $JC = 2.9533$, a very small energy gap that contributes to the low cost for this transfer. The servicer spends one revolution, or 71.75 days, along the customer orbit before returning to the depot on the operating orbit via the inbound leg of the homoclinic connection. A periodic transfer with an L_2 Lyapunov operating orbit at $JC = 2.9532$ and a customer orbit at $JC = 2.9573$ is available if two revolutions of the customer orbit are planned, corresponding to 13 revolutions of the 25.17-day operating orbit. Additional transfers are available if more revolutions along the customer orbit are desired.

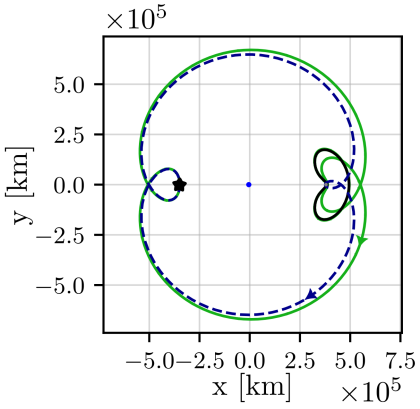

Figure 15: Periodic transfer from an L_2 Lyapunov orbit (black) to a 2:3 resonant orbit (blue, dashed) using a homoclinic connection with 2:3 resonance structure (green)

Homoclinic connections with resonant structure can be leveraged to transfer to different resonant orbits as well. As an illustrative example, in Figure 16 a transfer from a L_2 Lyapunov operating orbit to a customer's 1:2 resonant orbit using a homoclinic connection with 2:3 resonance structure is shown. The transfer cost is $\Delta v = 102.7 m/s$, higher than the previous examples due to the homoclinic connection and resonant orbit no longer sharing a common resonant structure. The operating orbit has an energy level of $JC = 2.961$ and the customer orbit is at an energy of $JC = 2.932$ where the servicer stays in the customer orbit for two revolutions for a servicing time of 109.7 days and a total time-of-flight of 288.9 days.

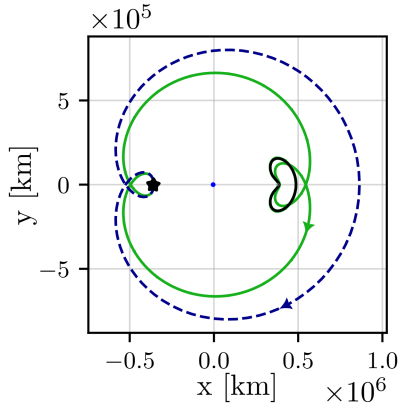

Figure 16: Periodic transfer from a L_2 Lyapunov (black) to a 1:2 resonant orbit (blue, dashed) using a homoclinic connection with 2:3 resonance structure (green)

Periodic transfers to stable orbits are also enabled, that is of particular interest as several spacecraft are placed into stable resonant orbits to leverage of their long-term stability. One such set of orbits is the stable 2:1 resonant orbits, that differ from the unstable members of the 2:1 family plotted in Figure 3(c) by being aligned with the y-axis rather than the x-axis.

Notably, Broucke[17] has demonstrated that both the stable and unstable 2:1 families are, in fact, part of the same family. However, for this analysis, they are differentiated based on their stability and geometry. A spatial stable 2:1 resonant orbit is the selected operating orbit for TESS, providing motivation for a servicing mission that can access such an orbit.

A periodic transfer from an L_2 Lyapunov to a stable 2:1 resonant orbit appears in Figure 17. The stable 2:1 orbits include periapses on the x-axis and some members include close approaches with the Earth, thus, a 3:1 resonant orbit structure is leveraged to transfer from the operating orbit to the 2:1 stable resonant orbit. The operating orbit has an energy level of $JC = 2.9954$, and the customer orbit energy equals $JC = 2.5152$, for a total transfer cost of $\Delta v = 129.3 m/s$. The servicer spends 1 revolution along the 2:1 orbit, corresponding to a servicing time of 27.31 days, and the transfer offers a time-of-flight of 221.23 days, corresponding to 11 revolutions of the 20.1-day operating orbit.

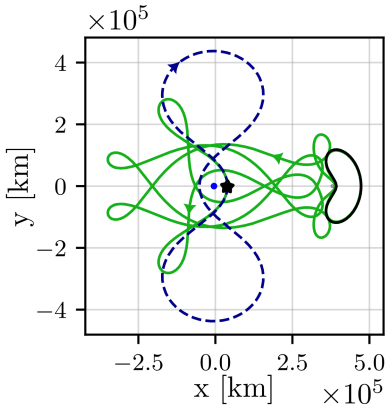

Figure 17: Periodic transfer from an L_2 Lyapunov orbit (black) to a 2:1 stable resonant orbit (blue, dashed) using a homoclinic connection with 3:1 resonance structure (green)

L_3 Lyapunov Orbits as Destinations

Compared to the L_1 and L_2 Lyapunov families, orbits in the vicinity of L_3 are less frequently the focus. However, Davis et al.[18] describe some advantages for using L_3 Lyapunov orbits for mission design, e.g., the ability to view nearly 50% of the Earth's surface at one time and low station-keeping requirements. Reaching L_3 Lyapunov orbits from the Lunar region also serves as a relevant case study to demonstrate the use of resonant structures to design periodic transfers that reach a variety of destinations in the Earth-Moon system.

An exterior resonant orbital structure for the homoclinic connection is advantageous for reaching L_3, as many of these orbits include motion in the vicinity of L_3 with a perpendicular crossing that matches the velocity direction for an L_3 Lyapunov orbit at that location. For example, a 4:5 resonant structure is used to create a periodic transfer from an L_2 Lyapunov orbit to an L_3 Lyapunov orbit and is plotted in Figure 18(a). The operating orbit energy level equals $JC = 2.941$ and the customer orbit energy is 2.991, with a total cost $\Delta v = 150.82 m/s$. The servicer spends 1 revolution along the customer orbit, with a period of 27.01 days, and the time-of-flight for the transfer is 270.3 days, equal to 10 revolutions of the 27.03-day operating orbit. Note that both the customer orbit, the operating orbit, and the homoclinic connection transfer time occur in a nearly 1:1:8 resonance between each segment and the Moon. As a result, the JC value for the operating orbit is nearly unchanged if additional revolutions of the customer orbit are incorporated, as $\mathcal{Q}$ remains very close to an integer if n_{PO} is varied. Figure 18(b) illustrates this phenomenon; as n_{PO} is varied, the energy level of the operating orbit remains nearly unchanged, with small variances in JC required to accommodate that the operating orbit, customer orbit, and homoclinic connection are not in perfect resonance with one another. The resonance between the different elements of the transfer adds versatility to a spacecraft servicing scenario, as the servicer could potentially spend an arbitrary number of revolutions on the customer orbit before returning due to the fact that the transfer is nearly unchanged as n_{PO} is increased.

It is possible to reach L_3 Lyapunov orbits of different sizes by adjusting the type of resonant structure that serves as the basis for the homoclinic connection. A homoclinic connection using a resonant structure with a smaller loop around L_3, such as a 2:3 resonant structure, delivers the servicer to a smaller L_3 Lyapunov orbit. Two transfers linking an L_2 Lyapunov operating orbit to an L_3 Lyapunov customer orbit using a homoclinic connection with an 2:3 resonant structure appear in Figures 19(a) and 19(c). The first transfer, in Figure 19(a), also exploits the near 1:1:6 resonance of the operating orbit, customer orbit, and homoclinic connection, as their respective periods are 27.57 days, 27.01 days, and 166.0 days, respectively. The transfer cost is $\Delta v = 205.04 m/s$ and the time-of-flight for a transfer incorporating 1 revolution along the customer orbit is 220.58 days, corresponding to 8 revolutions of the operating orbit. The required operating orbit JC value, if n_{PO} is varied, is plotted in Figure 19(b), where small variations in JC are required if n_{PO} is adjusted to maintain the periodicity of the transfer. Larger variations are required as compared to the transfer in Figure 18 due to the fact that the resonance between the operating orbit, customer orbit, and homoclinic transfer are not as close of an integer ratio.

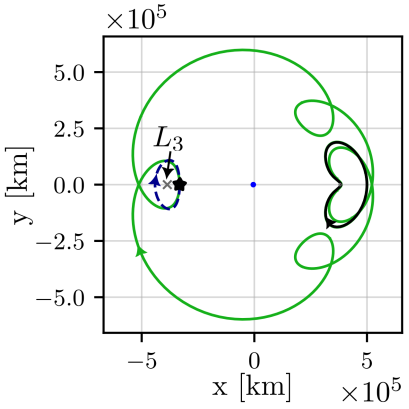

(a) Periodic transfer from an L_2 Lyapunov orbit (black) to an L_3 Lyapunov orbit (blue, dashed) using a 4:5 resonant structure (green)

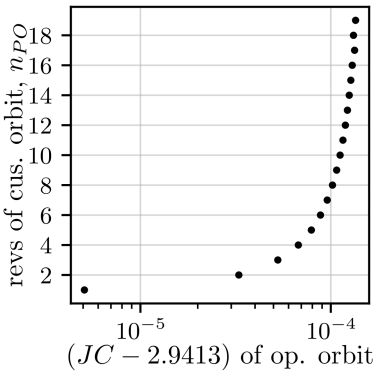

(b) Variation in the operating orbit JC required for a periodic transfer with n_{PO} revolutions of an L_3 Lyapunov

Figure 18: Periodic transfer from L_2 to L_3 Lyapunov orbit using 4:5 resonant structure

The second transfer, in Figure 19(c), uses an operating orbit with a higher energy level to reach an even smaller L_3 Lyapunov customer orbit. Recall that the periods along the L_3 Lyapunov family do not exhibit much variation relative to the Lunar period T_{moon} due to the 1:1 resonance with the Moon, therefore, the customer orbit results in a period of roughly one sidereal month. However, a periodic transfer with a smaller JC value for the operating orbit results in a period no longer close to a sidereal month as the period of the L_2 Lyapunov orbits varies with Jacobi Constant. The periodic transfer is, therefore, more sensitive to the number of revolutions of the customer orbit, as varying n_{PO} in Equation (6) results in a larger change in the operating orbit's Jacobi Constant value (and, therefore, the customer orbit's Jacobi Constant value) to converge to a periodic transfer. The energy level for the 21.98-day operating orbit and the customer orbit are $JC = 2.977$ and $JC = 3.01$, respectively, and this transfer results in a cost of $\Delta v = 220.7 m/s$. The servicer spends one revolution along the 27.0-day customer orbit and the total time-of-flight for the transfer is 197.97 days.

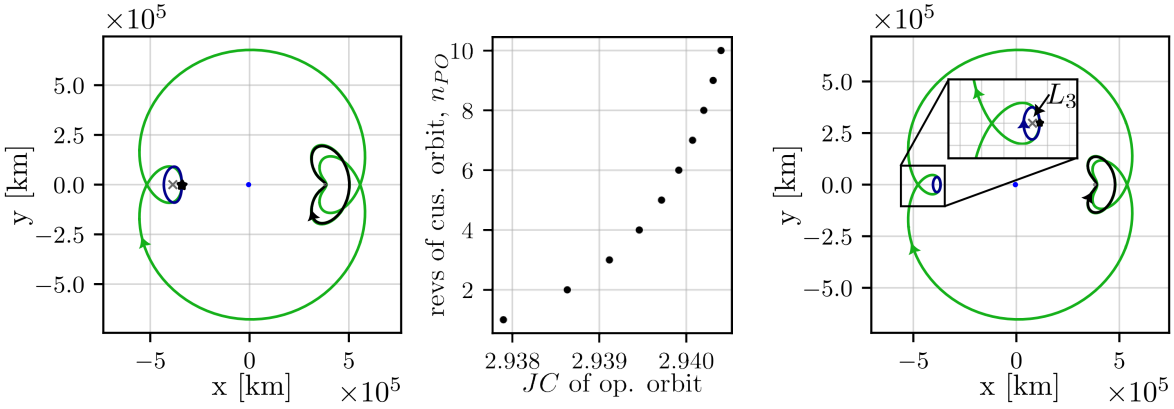

(a) Transfer where the operating orbit and customer orbit are in a near 1:1 resonance

(b) Operating orbit JC required for periodic transfers with n_{PO} revolutions of an L_3 Lyapunov for an L_2 Lyapunov orbit with near 1:1 Lunar resonance

(c) Transfer to a smaller L_3 Lyapunov

Figure 19: Periodic transfers from an L_2 Lyapunov orbit (black) to an L_3 Lyapunov orbit (blue) using some 2:3 resonant structure (green)

CONCLUDING REMARKS

Low-cost periodic transfers from an L_1 or L_2 Lyapunov operating orbit are generated to support crucial mission applications for the development of cislunar space. A transfer framework is proposed that uses ballistic transfers from the operating orbit with resonant structures for propellant-free departures from and arrivals into an operating orbit, with an optional insertion into a periodic resonant orbit at a perpendicular crossing. Natural parameter continuation for homoclinic connections yields a family of transfers with similar underlying resonant structures whose members are evaluated for the existence of a periodic transfer. The use of resonant structures is advantageous for access to many regions of cislunar space from the Lunar vicinity with low variance in their periods across the family, nearly ensuring the construction of a periodic transfer that reaches a desired region of space.

Numerous examples of periodic transfers with applications to space infrastructure are provided. Periodic transfers are potentially composed of a single homoclinic connection to permit a spacecraft to depart its operating orbit and eventually return without expending any propellant. Applications that may benefit from such a transfer are spacecraft collecting data in the Lunar region and a near-Earth pass to downlink data more easily.

Periodic transfers for a spacecraft servicing application are also created. Such a transfer is necessary for a framework that maintains a depot in the operating orbit with a servicer that departs the depot, offers services to a spacecraft, and returns to the depot to be replenished for another mission foray. Transfers that leverage a homoclinic connection to transfer the servicer to the customer's orbit quire low Δv magnitudes if the homoclinic connection and the customer orbit employ the same resonance structure. Transfers to orbits with different resonance structures are also possible, including transfers into stable resonant orbits. Finally, transfers to L_3 Lyapunov orbits are also constructed, and the low variation in the 1:1 resonance across the family is used to create transfers where the

operating orbit, homoclinic connection, and customer orbit are in a near-perfect resonance with one another, creating versatile transfer opportunities where the servicer potentially remains in the customer orbit for a nearly arbitrary number of revolutions, without the energy level of the transfer shifting significantly.

ACKNOWLEDGEMENTS

The authors appreciate the financial support provided by the Purdue University School of Engineering Education and the computational facilities in the Rune and Barbara Eliasen Visualization Laboratory. The first author would like to thank the *Fonds de Recherche du Québec – Nature et Technologies* for support through grant number 303482. Special thanks to Nicholas B. LaFarge and Rolfe J. Power for creating and sharing C++ integration tools. Finally, insightful discussions with fellow members of the Purdue Multi-Body Dynamics Research Group were greatly appreciated.

REFERENCES

[1] N. T. Redd, "Bringing Satellites Back From the Dead: Mission Extension Vehicles Give Defunct Spacecraft a New Lease on Life - [News]," *IEEE Spectrum*, Vol. 57, No. 8, 2020, pp. 6–7, https://doi.org/10.1109/MSPEC.2020.9150540.

[2] NASA's Exploration and In-space Services, "On-Orbit Satellite Servicing Study," tech. rep., National Aeronautics and Space Administration, Greenbelt, MD, USA, October 2010.

[3] A. Pasquale, G. Zanotti, J. Prinetto, M. Ceresoli, and M. Lavagna, "Cislunar distributed architectures for communication and navigation services of lunar assets," *Acta Astronautica*, Vol. 199, Oct. 2022, pp. 345–354, https://doi.org/10.1016/j.actaastro.2022.06.004.

[4] V. Szebehely, *Theory of Orbits: The Restricted Problem of Three Bodies*. Academic Press, 1967.

[5] M. Vaquero and K. C. Howell, "Leveraging Resonant-Orbit Manifolds to Design Transfers Between Libration-Point Orbits," *Journal of Guidance, Control, and Dynamics*, Vol. 37, July 2014, pp. 1143–1157, https://doi.org/10.2514/1.62230.

[6] M. Gupta and K. C. Howell, "Long-Term Cislunar Surveillance Via Multi-Body Resonant Trajectories," *AAS/AIAA Astrodynamics Specialist Conference*, August 2022.

[7] W. S. Koon, M. W. Lo, J. E. Marsden, and S. D. Ross, *Dynamical Systems, the Three-Body Problem, and Space Mission Design*. California Institute of Technology, 3rd ed., Apr. 2011.

[8] A. L. Batcha, J. Williams, T. F. Dawn, J. P. Gutkowski, M. V. Widner, S. L. Smallwood, B. J. Killeen, and R. E. Harpold, "Artemis I Trajectory Design and Optimization," *AAS/AIAA Astrodynamics Specialist Conference*, Virtual, 2020.

[9] D. Dichmann, J. Parker, C. Nickel, and S. Lutz, "Trajectory Design Enhancements to Mitigate Risk for the Transiting Exoplanet Survey Satellite (TESS)," *NASA Center for AeroSpace Information (CASI). Conference Proceedings*, Hampton, United States, NASA/Langley Research Center, Sept. 2016.

[10] A. F. Haapala and K. C. Howell, "A Framework for Constructing Transfers Linking Periodic Libration Point Orbits in the Spatial Circular Restricted Three-Body Problem," *International Journal of Bifurcation and Chaos*, Vol. 26, May 2016, p. 1630013. Publisher: World Scientific Publishing Co., https://doi.org/10.1142/S0218127416300135.

[11] J. S. Parker, K. E. Davis, and G. H. Born, "Chaining periodic three-body orbits in the Earth–Moon system," *Acta Astronautica*, Vol. 67, Sept. 2010, pp. 623–638, https://doi.org/10.1016/j.actaastro.2010.04.003.

[12] C. D. Murray and S. F. Dermott, *Solar System Dynamics*. Cambridge: Cambridge University Press, 2000, https://doi.org/10.1017/CBO9781139174817.

[13] R. L. Anderson, S. Campagnola, and G. Lantoine, "Broad search for unstable resonant orbits in the planar circular restricted three-body problem," *Celestial Mechanics and Dynamical Astronomy*, Vol. 124, Feb. 2016, pp. 177–199, https://doi.org/10.1007/s10569-015-9659-7.

[14] M. Gupta, K. C. Howell, and C. Frueh, "Earth-Moon Multi-Body Orbits to Facilitate Cislunar Surveillance Activities," *AAS/AIAA Astrodynamics Specialist Conference*, 2021.

[15] M. Vaquero and K. C. Howell, "Transfer Design Exploiting Resonant Orbits and Manifolds in the Saturn–Titan System," *Journal of Spacecraft and Rockets*, Vol. 50, No. 5, 2013, pp. 1069–1085, https://doi.org/10.2514/1.A32412.

[16] J. Casoliva, J. M. Mondelo, B. F. Villac, K. D. Mease, E. Barrabes, and M. Olle, "Two Classes of Cycler Trajectories in the Earth-Moon System," *Journal of Guidance, Control, and Dynamics*, Vol. 33, Sept. 2010, pp. 1623–1640, https://doi.org/10.2514/1.46856.

[17] R. A. Broucke, "Periodic Orbits in the Restricted Three-Body Problem With Earth-Moon Masses," Technical Report 32-1168, Jet Propulsion Laboratory, Pasadena, California, Feb. 1968.

[18] K. Davis, G. Born, M. Deilami, A. Larsen, and E. Butcher, "Transfers to Earth-Moon L3 halo orbits," *AIAA/AAS Astrodynamics Specialist Conference*, Vol. 152, Jan. 2012, https://doi.org/10.2514/6.2012-4593.